Final Draft

of the original manuscript

Bessa-Gonçalves, M.; Silva, A.; Brás, J.; Helmholz, H.; Luthringer-Feyerabend, B.; Willumeit-Römer, R.; Barbosa, M.; Santos, S.:
Fibrinogen and magnesium combination biomaterials modulate macrophage phenotype, NF-kB signaling and crosstalk with mesenchymal stem/stromal cells.
In: Acta Biomaterialia. Vol. 114 (2020) 471 - 484.

First published online by Elsevier: 18.07.2020

https://dx.doi.org/10.1016/j.actbio.2020.07.028

Fibrinogen and magnesium combination biomaterials modulate macrophage phenotype, NF-kB signaling and crosstalk with mesenchymal stem/stromal cells

Mafalda Bessa-Gonçalves[a,b], Andreia M. Silva[a,b], João P. Brás[a,b], Heike Helmholz[c], Bérengère J.C. Luthringer-Feyerabend[c], Regine Willumeit-Römer[c], Mário A. Barbosa[a,b], Susana G. Santos[a,b*]

[a]i3S – Instituto de Investigação e Inovação em Saúde, and INEB - Instituto de Engenharia Biomédica, Universidade do Porto, Rua Alfredo Allen 208, 4200-135 Porto, Portugal.

[b]Instituto Ciências Biomédicas Abel Salazar da Universidade do Porto, Rua de Jorge Viterbo Ferreira 228, 4050-313 Porto, Portugal.

[c]Helmholtz-Center Geesthacht, Centre for Materials and Coastal Research, Institute of Materials Research, Division for Metallic Biomaterials, Max-Planck-St.1, D-21502, Geesthacht, Germany

*Corresponding author.
i3S – Instituto de Investigação e Inovação em Saúde, Universidade do Porto
Rua Alfredo Allen, 208, 4200-135 Porto, Portugal.
E-mail address: susana.santos@ineb.up.pt (Susana G. Santos)

Abstract

Macrophage behavior upon biomaterial implantation conditions the inflammatory response and subsequent tissue repair. The hypothesis behind this work was that fibrinogen (Fg) and magnesium (Mg) biomaterials, used in combination (FgMg) could act synergistically to modulate macrophage activation, promoting a pro-regenerative phenotype. Materials were characterized by scanning electron microscopy, Fg and Mg degradation products were quantified by atomic absorption spectroscopy and ELISA. Whole blood immune cells and primary human monocyte-derived macrophages were exposed to the biomaterials extracts in unstimulated (M0) or pro-inflammatory LPS or LPS-IFNγ (M1) conditions. Macrophage phenotype was evaluated by flow cytometry, cytokines secreted by whole blood cells and macrophages were measured by ELISA, and signaling pathways were probed by Western blotting. The secretomes of macrophages preconditioned with biomaterials extracts were incubated with human mesenchymal stem/stromal cells (MSC) and their effect on osteogenic differentiation was evaluated *via* Alkaline Phosphatase (ALP) activity and alizarin red staining. Scaffolds of Fg, alone or in the FgMg combination, presented similar 3D porous architectures. Extracts from FgMg materials reduced LPS-induced TNF-α secretion by innate immune cells, and macrophage M1 polarization upon LPS-IFNγ stimulation, resulting in lower cell surface CD86 expression, lower NFκB p65 phosphorylation and reduced TNF-α secretion. Moreover, while biomaterial extracts *per se* did not enhance MSC osteogenic differentiation, macrophage secretome, particularly from cells exposed to FgMg extracts, increased MSC ALP activity and alizarin red staining, compared with extracts alone. These findings suggest that the combination of Fg and Mg synergistically influences macrophage pro-inflammatory activation and crosstalk with MSC.

Keywords: biomaterials; fibrinogen; magnesium; macrophages; mesenchymal stem/stromal cells

Statement of significance

Modulating macrophage phenotype by degradable and bioactive biomaterials is an increasingly explored strategy to promote tissue repair/regeneration. Fibrinogen (Fg) and magnesium (Mg)-based materials have been explored in this context. Previous work from our group showed that monocytes interact with fibrinogen adsorbed onto chitosan surfaces through TLR4 and that fibrinogen scaffolds promote *in vivo* bone regeneration. Also, magnesium ions have been reported to modulate macrophage pro-inflammatory M1 stimulation and to promote bone repair. Here we report, for the first time, the combination of Fg and Mg materials, hypothesizing that it could act synergistically on macrophages, directing them towards a pro-regenerative phenotype. As a first step towards proving/disproving our hypothesis we used extracts obtained from Fg, Mg and FgMg multilayer constructs. We observed that FgMg extracts led to a reduction in the polarization of macrophages towards a pro-inflammatory phenotype. Also, the secretome of macrophages exposed to extracts of the combination material promoted the expression of osteogenic markers by MSCs.

1. Introduction

Inflammation is necessary for adequate and complete bone healing upon injury, but exacerbated inflammation underlies most musculoskeletal diseases [1]. While fracture-related injury elicits a beneficial acute inflammatory response, chronic inflammation impairs bone health and repair [1].

Thus, biomaterials capable of modulating the inflammatory response have been increasingly explored to promote tissue repair/regeneration [2]. Monocytes/macrophages are a central cell population in biomaterials response, conditioning inflammatory and regenerative processes, by transitioning between pro- (M1) and anti-inflammatory (M2) phenotypes [3]. Polarizing macrophages towards an M2 phenotype is a strategy that impacts on recruitment of Mesenchymal Stem/Stromal Cells (MSC) via paracrine factors [4, 5], leading to their osteogenic differentiation [4, 5].

Fibrinogen (Fg) is a protein with essential roles in coagulation, wound healing and inflammation. Its healing properties are well known and are the basis for wide use of fibrin glue [6]. On the other hand, its pro-inflammatory impact has been described in several diseases, like Alzheimer's, Stroke, or Rheumatoid Arthritis [7]. Previous work from our group showed that Fg adsorbed to chitosan interacts with monocytes through TLR4 [8], enhances the production of osteogenic factors by macrophages [9], and MSC recruitment by natural killer (NK) cells [10]. In addition, in a femoral bone defect model, Fg adsorbed to chitosan [11] or as pure Fg scaffolds [12] modulated local and systemic response to injury, both at 6 days (end of acute inflammation) and 8 weeks (repair/remodeling stage) post-injury, improving bone repair [12].

On the other hand, Magnesium (Mg) alloys are promising biomaterials for orthopedic applications, due to their mechanical properties similar to human bone, degradability and the physiological role of Mg in bone [13]. However, the use of Mg alloys is limited by their fast degradation rate, which leads to the release of high amounts of metallic ions, substantial pH increase and generation of hydrogen gas, all with adverse tissue

effects. This destabilizes the bone-implant interface and hinders healing [13, 14]. Interestingly, at low concentration Mg degradation products may have beneficial effects in modulating the immune response, and promoting MSC proliferation and osteogenic differentiation [15, 16]. To tailor Mg biomaterials degradation rate and biocompatibility, alloying elements and subsequent thermal or mechanical treatment have been explored [17, 18]. Also, combining Mg biomaterials with degradable polymers could be an attractive option, to gain greater control over biodegradability and promotion of fully functional remodeled bone tissue [14, 18].

Herein, we hypothesize that the combination of Fg and Mg into the same biomaterial can act synergistically to modulate macrophage activation and their crosstalk with MSC. To test this hypothesis, pure fibrinogen scaffold (denoted as "Fg"), Mg discs ("Mg") and multilayer constructs combining Fg and Mg ("FgMg") were prepared. Instead of seeding cells directly on these biomaterials we have used their extracts. The potential of Fg, Mg and FgMg extracts to modulate the phenotype of macrophages, and the impact of their secretome on MSC differentiation were evaluated. Results show, for the first time, that FgMg material extracts were capable of reducing M1 polarization in primary macrophages, leading them to produce a secretome that promoted MSC osteogenic differentiation.

2. Materials and Methods

2.1. Biomaterial formulations

2.1.1. Fg scaffolds: Fg 3D scaffolds (12 mm diameter x 9 mm thickness) (Supplementary Fig.1) were prepared by freeze-drying, as previously described [12]. Briefly, a solution of Fg 60 mg/mL (from human plasma, Grifols S.A., Barcelona, Spain) was prepared from an 80 mg/mL Fg stock solution, in water, and cast into 48-well plates (1000 μL/well), frozen overnight (o.n.) at -20 ºC, and freeze-dried for 48 h, at -80

ºC. Resulting scaffolds were chemically crosslinked o.n. with N-(3-Dimethylaminopropyl)-N′-ethylcarbodiimide hydrochloride (EDC, E1769, Sigma-Aldrich Co., St Louis, MO, USA) at 8.8 mM, prepared in ethanol, as described [19]. Then, scaffolds were removed from the plate, neutralized and disinfected, through impregnation under vacuum in a gradient of ethanol solutions (99.9%, 70%, 50% and 25%), followed by three washes in cell culture media.

2.1.2. Mg discs: Pure Mg ingots (Mg; 99.95%) were prepared by permanent mould gravity casting at Helmholtz Zentrum Geesthacht (Geesthacht, Germany). After extrusion, 10 mm diameter x 1.5 mm thickness discs were cut from rods, as described in [20]. The discs (Supplementary Fig.1) were cleaned by sonication for 20 min in n-hexane (Merck, Darmstadt, Germany), for 20 min in acetone (Merck, Darmstadt, Germany) and for 3 min in 100% ethanol. Lastly, specimens were sterilized in 70% ethanol (20 min with sonication) and dried under sterile conditions [20]. Degradation rate of the current batch of Mg discs (Mg pure 16614) was determined prior to *in vitro* tests. The degradation rate, 0.32 mm/year, was measured in media supplemented with FBS, during 7 days immersion, and under cell culture conditions (37 ºC, 21% O2, 5% CO2, 95% RH), as previously described in [21].

2.1.3. Fg scaffolds combined with Mg discs (multilayer constructs)**:** a solution of Fg 60 mg/mL (from human plasma, Grifols S.A., Barcelona, Spain) prepared as above was cast into 48-well plates (500 μL/well) and frozen o.n. at -20 ºC. Mg discs were cleaned as above, cooled (-20ºC), and placed on top of the Fg layer. Then, another layer of Fg (500 μL) was added on top of the Mg disc. Resulting multilayer constructs (Supplementary Fig.1) (a total of three layers (Fg-Mg-Fg), with combined 12 mm diameter x 10,5 mm thickness (each Fg layer with 4,5 mm thickness and Mg disc with 1,5 mm thickness)) were frozen, freeze-dried and then chemically crosslinked and processed as described above for Fg scaffolds.

2.2 Scanning electron microscopy (SEM) and energy dispersive spectroscopy (EDS) characterization

Microstructure/surface morphology of Fg alone or in the FgMg combination was analysed by SEM/EDS using a high resolution (Schottky) environmental EM with X-ray microanalysis and electron backscattered diffraction analysis (Quanta 400 FEG ESEM / EDAX Genesis X4M). Cross-sections of approximately 1 mm thickness were cut and mounted with carbon tape. Samples were coated with a gold (Au)/ palladium (Pd) thin film, by sputtering for 80 sec with 15 mA current, to provide conductivity, using the SPI module sputter coater equipment [12]. EDS coupled to SEM was used for elemental analysis.

2.3. Extracts preparation and characterization

Extracts were prepared according to EN ISO standards 10993:5 (ISO 10993-5:2009) and 10993:12 (ISO 10993-12:2012), using 0.1 g material/mL extraction medium for Fg and 0.2 g material/mL extraction medium for Mg and FgMg. After sterilization, samples were incubated in extraction media (Roswell Park Memorial Institute (RPMI) 1640 media with L-glutamine, Corning, Manassas, USA), supplemented with 10% fetal bovine serum (FBS) (Biowest, Riverside, MO, USA) for 72 h at 37 ºC with 120 rpm agitation. pH measurements were performed using an ArgusX pH Meter (Sentron Europe BV, Roden, the Netherlands) for pure Fg, Mg, and FgMg extracts, and RPMI cell culture media, as control. Mg content on elutes (mg/L) was measured *via* atomic absorption spectroscopy (AAS; Agilent 240 AA, Waldbronn, Germany). An external calibration was performed for quantification, which uses Mg reference solution to cover the targeted analyte range (element-specific detections at absorbance 285.2 nm). Air/Acetylene flame type together with pre-read delay time of 3 seconds and a read time of three seconds with three replicates were used. Fg degradation product D-dimer was quantified by enzyme-linked immunosorbent assay (ELISA), using RayBio®

Human D-Dimer ELISA Kit (RayBiotech, Norcross, GA, USA), according to manufacturer's instructions. A calibration curve using standards was used to quantify the relative amount of D-Dimer in each sample. Before being used for cell culture experiments, pure extracts were diluted (1:10) in fresh RPMI 1640 media, complete with L-glutamine (Corning, Manassas, USA), and supplemented with 10% fetal bovine serum (FBS, Biowest, Riverside, MO, USA), using methods adapted from [15], and pH measurements upon extracts dilution were performed as above.

2.4. Ethics statement

All obtained human samples and procedures were performed in agreement with the principles of the Declaration of Helsinki. Monocytes were isolated from surplus buffy coats (BC) from healthy blood donors, kindly donated by *Serviço de Imunohemoterapia, Centro Hospitalar Universitário de São João* (CHUSJ), Porto. Human mesenchymal stem/stromal cells (MSC) were obtained from healthy human bone marrow from patients undergoing knee ligament surgery, kindly donated by *Serviço de Ortopedia,* CHUSJ, Porto. All experimental protocols were conducted following the approval and recommendations of the CHUSJ Ethics Committee for Health (references 90/19 and 260/11). Buffy coats and bone marrow samples were provided anonymized and patient identification was not provided to researchers.

2.5. Whole blood innate immune stimulation

Buffy coats from peripheral blood of healthy blood donors were cultured for 24h (200 µl per well) with Fg, Mg and FgMg extracts (diluted 1:10, as described in 2.3), in presence or absence of 10 ng/mL LPS, Escherichia coli O55:B5 (Sigma-Aldrich Co., St Louis, MO, USA), following protocols adapted from [22]. After incubation, the bloods were centrifuged for 2 min, 10000 *g*, RT (Heraeus™ Fresco™ 21 Microcentrifuge,

ThermoFisher Scientific, Waltham, MA, USA) and supernatants were collected. The effect on Human tumor necrosis factor α (TNF-α), secretion was investigated by ELISA (ELISA Max™ Deluxe, BioLegend, San Diego, CA, USA) according to manufacturer's instructions [12].

2.6. Primary human monocyte isolation and macrophage differentiation

Human monocytes were isolated from peripheral blood of healthy blood donors by negative selection, using methods described in [8]. Briefly, BC were centrifuged at room temperature (RT) for 20 min at 1200 g (Eppendorf Centrifuge 5810R, VWR International LLC, Radnor, PA, USA), without active acceleration or brake, for blood components separation. Peripheral blood mononuclear cells (PBMC) were collected and incubated with RosetteSep™ Human Monocyte Enrichment Cocktail (StemCell Technologies, Vancouver, Canada) at RT for 20 min under gentle mixing. The mixture was then diluted at a 1:1 ratio with 2% heat inactivated FBS (Biowest, Riverside, MO, USA) in PBS, gently layered over Histopaque-1077 (Sigma-Aldrich Co., St Louis, MO, USA) and centrifuged as previous. The enriched monocyte layer was collected and washed three times with PBS by centrifugation at 17 min, 700 rpm, RT (Eppendorf Centrifuge 5810R, VWR International LLC, Radnor, PA, USA).

For macrophage differentiation, 0,5 x 10^6 monocytes were seeded on glass coverslips in 24-well plates, and cultured for 7 days in RPMI 1640 media with L-glutamine (Corning, Manassas, VA, USA) supplemented with 10% heat-inactivated FBS (Biowest, Riverside, MO, USA), 100 U mL^{-1} penicillin and 100 µg/mL^{-1} streptomycin (P/S, both from Invitrogen, Carlsbad, CA, USA), in the presence of 50 ng/mL of recombinant human macrophage colony-stimulating factor (rh M-CSF, ImmunoTools, Friesoythe, Germany). After 7 days, cell culture media was replaced and M-CSF was removed. At day 10, media was replaced and monocytes/macrophages were stimulated with 10

ng/mL LPS, (as above) and 50 ng/mL IFNγ (ImmunoTools, Friesoythe, Germany), for M1, in presence or absence of Fg, Mg and FgMg extracts (diluted 1:10, as described in 2.3), for 72h. Supernatants were collected under sterile conditions at day 13, centrifuged at 13,000 rpm, 5 min, 4 ºC (Eppendorf Centrifuge 5810R, VWR International LLC, Radnor, PA, USA), to remove any cellular debris, and stored at -20 ºC until further analysis, or used to prepare conditioned media for MSC cultures. Macrophages were then incubated with PBS-50 mM ethylenediaminetetraacetic acid (EDTA, VWR International LLC, Radnor, PA, USA) during 15 min at 4 ºC and gently harvested for further experiments. The complete experimental procedure is described in Fig. 1.

2.7. Macrophage polarization evaluation by flow cytometry

Macrophages collected at day 13, were washed, resuspended in FACS buffer (PBS, 2% FBS, 0.01% sodium azide (Sigma-Aldrich Co., St Louis, MO, USA) and stained with specific fluorochrome-conjugated antibodies, in the dark, for 30 min at 4 °C. Macrophages were incubated with the following antibodies: anti-human CD14-APC (clone MEM-18), CD86-FITC (clone BU63) (all from ImmunoTools, Friesoythe, Germany) and CD163-PE (clone GHI/61) (BD Biosciences, San Jose, CA, USA). Isotype-matched antibodies were used as negative controls, to define background staining. After additional washes, 10,000 cells, gated according to forward and side scatter parameters, were acquired using a BD FACSCanto II™ flow cytometer (Becton Dickinson) using FACSDiva™ software (both from BD Biosciences, San Jose, CA, USA). Data were analysed using FlowJo software (BD Biosciences, San Jose, CA, USA, version 10) and the percentage of CD14, CD86 and CD163 positive cells was calculated by subtracting the corresponding isotype control.

2.8. Western blot analysis

Macrophages were treated with Fg, Mg and FgMg biomaterial extracts (diluted 1:10, as described in 2.3) in the presence/absence of M1 stimulation (as above), for 30 min. Using methods described in [8], cells were harvested and washed twice with cold PBS, before cell lysis with RIPA buffer (1% NP-40 (Sigma-Aldrich Co., St Louis, MO, USA), 150 mM NaCl (VWR International LLC, Radnor, PA, USA), 50 mM Tris-HCl (pH 7.5) (Sigma-Aldrich Co., St Louis, MO, USA), 2 mM EDTA (VWR International LLC, Radnor, PA, USA)) supplemented with a mixture of phosphatase and protease inhibitors (10 µg/mL NaF (VWR International LLC, Radnor, PA, USA), 20 µg/mL Na_3VO_4, 10 µg/mL PMSF, 10 µg/mL aprotinin, 10 µg/mL leupeptin and 50 µg/mL $Na_4P_2O_7$ (all from Sigma-Aldrich Co., St Louis, MO, USA)) for 30 min, on ice, with frequent shaking. Lysates were collected, centrifuged at 14,000 rpm, 10 min, 4°C (Eppendorf Centrifuge 5810R, VWR International LLC, Radnor, PA, USA), and supernatants were recovered and stored at -80 °C until protein quantification using DC protein assay kit (Bio-Rad Laboratories, Irvine, CA, USA). The same amount of protein per sample (30 µg/lane) was resolved by SDS-PAGE in reducing conditions using 10% polyacrylamide gels, and transferred to nitrocellulose membranes (GE Healthcare, Chicago, IL, USA). Membranes were blocked in a solution of 5% bovine serum albumin (BSA, VWR International LLC, Radnor, PA, USA) in Tris-buffered saline (TBS)-Tween 0.1%, and then probed o.n. at 4 °C, using the following primary antibodies: phospho-p38 MAPK (dilution 1:1000; cat. no.4511); phospho-p44/42 MAPK (Erk1/2) (dilution 1:2000; cat. no.4370); phospho-SAPK/JNK (dilution 1:1000; cat. no.4668); phospho-NF-κB p65 (dilution 1:1000; cat. no.3033), glyceraldehyde 3-phosphate dehydrogenase (GAPDH - used as protein loading control; dilution 1:1000; cat. no.5174) (all from Cell Signalling Technology, Danvers, MA, USA). The secondary antibody used for signal detection was horseradish peroxidase (HRP)-conjugated goat anti-rabbit immunoglobulin (IgG) (dilution 1:2000; cat. no.7074, Cell Signalling Technology, Danvers, MA, USA). Blots

were visualized using a chemiluminescent substrate ECL Prime (GE Healthcare, Chicago, IL, USA) and exposure to X-ray films [8]. The films were scanned in a Molecular Imager GS-800 calibrated densitometer (Bio-Rad Laboratories, Irvine, CA, USA), and quantitative results were obtained using Image Lab (Bio-Rad Laboratories, Irvine, CA, USA, version 6.0.1), normalizing the values of each sample with the values of GAPDH.

2.9. Macrophage cytokine secretion profile by ELISA

The relative concentration of different cytokines was quantified (pg/mL) in macrophage culture supernatants from 72h stimulation, using commercially available ELISA kits. Human tumor necrosis factor α (TNF-α), interleukin (IL) -6, IL-1β, IL-12p70 and IL-10 (ELISA Max™ Deluxe, BioLegend, San Diego, CA, USA) [12], and human transforming growth factor β1 (TGF-β1) (DuoSet® ELISA development system, R&D systems, Minneapolis, Minnesota, USA) [23] ELISA were performed according to manufacturer's instructions.

2.10. Primary human mesenchymal stem/stromal cells isolation, culture and osteogenic differentiation

Primary human MSC were isolated from bone marrow by density gradient centrifugation followed by selection of adherent cells, and characterization according to the international stem cell society criteria, as previously described [10]. Bone marrow was collected from patients undergoing orthopaedic surgery. After lymphoprep gradient centrifugation at 1100 g, 30 min, 20ºC, without brake (Eppendorf Centrifuge 5810R, VWR International LLC, Radnor, PA, USA), cells were collected and plated in MSC growth medium (Dulbecco's modified Eagle's medium (DMEM) supplemented with 10% FBS Gibco MSC qualified (Fisher Scientific, Hampton, New Hampshire, USA) and 1%

P/S) [10]. For MSC culture and maintenance, cells were seeded in 175 cm^2 tissue culture flasks (Falcon, Corning, Manassas, USA) with Dulbecco's modified Eagle's medium (DMEM; low-glucose with glutamax Corning, Manassas, USA) supplemented with 10% FBS Gibco MSC qualified (Fisher Scientific, Hampton, New Hampshire, USA) and 1% P/S. Media was changed twice a week. Cells were passaged at 80% confluence by washing with warm PBS and detaching cells by using Gibco trypsin-EDTA 0.05% (Fisher Scientific, Hampton, New Hampshire, USA) for 5 min at 37 ºC. The viable cells were counted using trypan blue (Sigma-Aldrich Co., St Louis, MO, USA) exclusion dye and seeded at a density of 3000 cells/cm^2 in 175 cm^2 tissue culture flasks (Falcon, Corning, Manassas, USA).

For osteogenic differentiation assays MSC were used at passage 7 and a total of 6000 cells/cm^2 were seeded on 96-well plates and incubated at 37 ºC in DMEM supplemented with 10% FBS and 1% P/S. After reaching confluence, media was changed for: (i) negative control (basal media: DMEM (with 10% FBS and 1% P/S); (ii) positive control (osteogenic media: DMEM with 10% FBS (Biowest, Riverside, MO, USA), 1% P/S, 100 mM dexamethasone (Sigma-Aldrich Co., St Louis, MO, USA) , 0.05 mM ascorbic acid (Sigma-Aldrich Co., St Louis, MO, USA) and 10 mM β-glycerophosphate (Sigma-Aldrich Co., St Louis, MO, USA)); (iii) biomaterials extracts controls (Fg, Mg and FgMg extracts diluted 1:10, as described in 2.3, and then diluted 1:2 in basal media to have similar conditions as for conditioned media); and (iv) conditioned media from day 13 macrophages preconditioned with biomaterials extracts in presence/absence of M1 stimulation (as described in 2.6), diluted in basal media 1:2. For each condition, two replicates were made for colorimetric evaluation of ALP activity and calcium deposition (alizarin red staining). Media was changed twice a week maintaining the respective stimulation, until day 14.

2.11. ALP and Alizarin Red staining

Before ALP staining at day 14, MSC were washed twice with PBS and fixed with 4% paraformaldehyde (Sigma-Aldrich Co., St Louis, MO, USA). Then, fixed MSC were incubated with ALP substrate, composed by 4% naphtol AS-MX phosphate alkaline solution in Fast Violet B solution (both from Sigma-Aldrich Co., St Louis, MO, USA) for 45 min at RT [24]. Calcium deposition was assessed by staining fixed MSC with Alizarin Red S (AZ) (Sigma-Aldrich Co., St Louis, MO, USA) for 10 min at room temperature [24]. Samples were washed twice in PBS at 4 ºC and kept in water until being photographed under a stereomicroscope (Olympus SZX10, Shinjuku, Tokyo, Japan). The acquired images were analysed using an algorithm developed in MATLAB (Mathworks, Natick, MA, USA, version R2017b) to quantify ALP and AZ staining, as previously described [25]. In detail, ALP and AZ intensities were quantified after thresholding colour images on the total area of each well (ALP: red > 0.1; red > 0.9 x green; green< 0.92 x blue; AZ: red > 1.4 x green; red > 1.3 x blue).

2.12. Statistical analysis

Statistical analysis was performed using GraphPad Prism software (San Diego, CA, USA, version 7). Data were tested for normality using D'Agostino & Pearson normality test. To compare multiple groups Friedman's or Kruskal-Wallis tests were performed, followed by Dunn's multiple comparisons test for non-parametric data, while for parametric data ANOVA followed by Sidak's multiple comparisons test were used, as specified in figure legends. Data are represented as arithmetic mean ± standard deviation (SD) from at least three independent experiments. Error bars on box-and-whiskers plots indicate the minimum and maximum values obtained in the analysis. Statistical significance was considered for *p<0.05; **p<0.01; ***p<0.001; ****p<0.0001.

3. Results

3.1. Fg scaffolds and their combination with Mg discs: 3D architecture and extract composition

Fg scaffolds were produced by freeze-drying, as described before [12], and combined with Mg discs. First, we analyzed the morphology of the Fg layer (Fig. 2). The SEM analysis revealed that the interconnected porous structure of Fg was largely maintained in the FgMg materials (Fig. 2A). As expected, EDS analysis showed the presence of detectable amounts of Mg in the Fg layer, only when analysing the FgMg combination (Fig. 2B).

Next, material extracts were produced and their Mg and Fg composition was evaluated. AAS was used to measure Mg concentration, and results (Fig. 2C) showed, as expected, that extracts from Fg materials had only residual Mg content, and significantly less than those from Mg and FgMg materials, which contained an average of 122.8±10.11 and 205.8±30.05 mg/L of Mg, respectively. The presence of Fg degradation products was measured using the D-Dimer quantification kit. Extracts from Fg materials had slightly higher levels of D-dimer than those from FgMg materials, and both had significantly more D-dimer than the residual amounts detected in Mg materials extracts (Fig. 2D). The pH of the extract solutions was also determined and was higher in the extracts of Mg-containing biomaterials when compared with Fg-only ones, Fg (8.29 ± 0.02), Mg (9.80 ± 0.11) and FgMg (9.94 ± 0.02), and with RPMI cell culture media (7.81 ± 0.09). Upon 1:10 dilution, the pH of all extracts was in the physiologic range, 7.93 ± 0.15 for Fg, 8.31 ± 0.04 for Mg and 8.32 ± 0.02 for FgMg.

Overall, these results indicated that the presence of Mg discs still allows the formation of a porous 3D structure characteristic of Fg, but Mg is released and found in the Fg layer of combination materials. Concentrations of degradation products for Mg and Fg were not statistically different between the single material extract and the extract of the combination.

3.2. FgMg biomaterial extracts decreased LPS-stimulated TNF-α secretion

To evaluate the activation of innate immune cells and the potential for biomaterial extracts to act as immune-modulators, we first analyzed the impact of Fg, Mg and FgMg extracts, alone or upon endotoxin (i.e. LPS) stimulation, on concentrated whole blood, containing all peripheral blood immune cell populations. Results illustrated in Fig. 3 show that, none of the biomaterial extracts per se led to TNF-α secretion. As expected, secretion levels of TNF-α were significantly up-regulated in blood samples stimulated with LPS, comparing to non-stimulated samples. All extracts have shown the capacity to reduce TNF-α secretion levels, in response to LPS stimulation, but only extracts from the FgMg combination led to significantly less TNF-α secretion, when compared to the LPS stimulated control.

3.3. FgMg biomaterial extracts impaired macrophage M1 polarization

As macrophages play a central role in biomaterials response, next we sought to investigate in more detail whether macrophage polarization could be modulated by the degradation products from Fg, Mg or FgMg biomaterials. Macrophages were exposed to the materials extracts and either left unstimulated, or stimulated towards M1 pro-inflammatory phenotype, by the addition of LPS and IFNγ. Cell surface markers associated to M1 (CD86) and M2 phenotypes (CD163) were analyzed in relation to the lineage marker CD14, at day 13. Dot plots illustrating macrophage phenotype in the different conditions are presented in Fig. 4A. When the percentage of positive cells for each marker was quantified across different donors, high percentages of CD14 positive cells were found, as expected. M1 stimulation increased the percentage of CD14 cells, particularly when combined with the presence of FgMg extracts, leading that increase to be statistically significant, compared to the respective M0 control (Fig. 4B). The biomaterial extracts *per se* did not increased CD86 cell surface expression, as all M0

conditions show similar and low percentages of CD86 positive cells. M1 stimulation, with LPS-IFNγ, increased the percentage of cells expressing CD86 in control (CTRL) culture conditions and in the presence of extracts of Fg and Mg materials separately. Interestingly, in presence of extracts from the FgMg combination biomaterial, the percentage of CD86 positive cells was no longer significantly different from M0 unstimulated conditions (Fig. 4C). As expected, the percentage of cells expressing CD163 (M2 marker) decreased when cells were stimulated towards M1 polarization and results showed that the presence of the different biomaterial extracts did not have a significant impact on CD163 expression (Fig. 4D). The decrease in CD86 levels in M1 stimulated macrophages exposed to FgMg extracts suggests that this combination impairs M1 polarization.

3.4. FgMg biomaterial extracts decreased NF-kB p65 phosphorylation, following M1 stimulation

To uncover the mechanism by which the FgMg extract could be impairing the M1 activation of macrophages, the MAPK signalling pathways (JNK, ERK and p38) and NF-kB p65 phosphorylation, known to be stimulated in monocytes/macrophages in response to M1 stimulation [8, 26-28], were probed by Western blotting. Results depicted in Fig. 5 highlighted that biomaterial extracts *per se* did not induce activation of MAPK pathways or NF-kB p65 phosphorylation. As expected, activation of all MAPK pathways occurred in response to M1 stimulation. When results were quantified across different donors, we could observe a tendency for FgMg extracts to increase ERK and decrease p38 phosphorylation levels in the presence of M1 stimulation, albeit this observation was not statistically significant. Interestingly, the presence of materials extracts reduced phosphorylation levels of NF-kB p65, activated in response to M1 stimulation, reaching statistical significance for the FgMg combination extract. In conclusion, results showed that FgMg extracts lead to the downregulation of NF-kB

p65 phosphorylation, suggesting that this combination may have an impact over the inflammatory signaling pathways.

3.5. Fg, Mg and FgMg biomaterials extracts influenced cytokine secretion by M1 stimulated macrophages

Cytokines are important players in the inflammatory response to biomaterials and important regulators of its progression and resolution [29]. To explore the functional consequences of Fg, Mg and FgMg extracts on M0 and M1-stimulated macrophages, cytokine secretion profiles were assessed. Results presented in Fig. 6 show that biomaterial extracts *per se* had no significant impact on the secretion levels of TNF-α, IL-6, IL-1β, IL-12 p70, IL-10 or TGF-β1. As expected, in control conditions secretion levels of TNF-α, IL-6, IL-1β, IL-12p70 and IL-10 were up-regulated in M1 stimulated macrophages, comparing to their M0 counterparts. Interestingly, material extracts impacted cytokine secretion levels in response to M1 stimulation. While all material extracts reduced TNF-α secretion levels upon M1 stimulation, with loss of the statistically significant increase between M0 and M1 in presence of Fg and FgMg extracts, IL-6 secretion was only impacted by Mg material extract. Moreover, Fg extracts impaired the increased IL-1β secretion in response to LPS-IFNγ stimulation, compared to the respective M0, and showed significantly lower secretion, when compared with M1 in CTRL conditions. Secretion levels of IL-12p70 were not significantly increased by M1 stimulation when macrophages were in presence of Mg and FgMg extracts. Materials extracts did not impact the increased IL-10 secretion upon M1 stimulation, when compared with respective M0 macrophages. In addition, FgMg extracts significantly increased macrophage TGF-β1 secretion in response to M1 stimulation, when compared to their M0 counterparts. Overall, Fg, Mg and FgMg extracts led to decreased secretion of specific cytokines by M1-stimulated

macrophages which might point towards distinct immunomodulatory effect upon different cytokines.

3.6. Secretome from macrophages preconditioned with FgMg biomaterial extracts increased MSC ALP activity and calcium deposition

Next we wanted to evaluate the impact of the observed macrophage immunomodulation by the biomaterials extracts, on their crosstalk with MSC. So, the secretome produced by macrophages preconditioned with biomaterials extracts in the presence/absence of M1 stimulation, was used for promoting MSC osteogenic differentiation in the absence of osteoinductive stimulation (ascorbic acid, β-glycerophosphate and dexamethasone). MSC cultured in presence of Fg, Mg and FgMg extracts were used as controls, for the potential direct effect of biomaterials extracts on osteogenesis. Osteogenesis in presence of chemical inductors was used as positive control. ALP activity staining was performed at day 14, as an indicator of early osteogenesis. Results illustrated in Fig. 7A show the quantification of ALP-stained areas across the different experiments. In general, secretome from M1 stimulated macrophages promoted higher ALP activity than those of M0 macrophages, although the differences were not statistically significant. Interestingly, the secretome of macrophages exposed to FgMg extracts promoted the highest ALP activity, with that of M0 macrophages, inducing significantly higher ALP activity than the one from CTRL M0 macrophages, or from M0 exposed to Fg material extracts. When macrophage secretomes were compared to the biomaterial extracts *per se*, the secretome of M0 macrophages exposed to Mg extracts induced significantly higher ALP activity than Mg extracts, and secretomes of macrophages (M0 and M1) exposed to FgMg extracts induced higher ALP activity than FgMg extract.

Moreover, the effect of macrophages secretome on mineral deposition was analysed by alizarin red staining. Results presented in Fig. 7B show that, similarly to ALP

activity, materials extracts *per se* did not increase calcium deposition significantly, while more alizarin red staining could be observed in MSC stimulated by the secretome of macrophages. In general, macrophage exposure to biomaterials extracts led to secretomes that induced significant increases in alizarin red staining in MSC cultures, when compared to those exposed to extracts alone. Albeit, MSC cultured with secretome of M0 macrophages not exposed to any extract led to a significant increase in the alizarin red staining, compared to their M1 counterparts.

To determine the contribution of the materials degradation products, contained in macrophage secretome, for ALP activity and mineral deposition the concentration of Mg ions and Fg degradation product, D-dimer, in conditioned media was evaluated. The results obtained are presented in Fig. 8, and show similar Mg concentrations in the conditioned media of macrophages exposed to all extracts and control conditions, while Fg degradation product D-dimer was more concentrated in conditioned media from macrophages exposed to Fg and FgMg biomaterials. Together, these results indicated that the macrophage secretion products induced ALP activity and mineral deposition on MSC, while direct exposure to biomaterial degradation products did not have the same impact.

4. Discussion

Macrophages are key players in the inflammatory response to injury and to biomaterial implantation [2], and their modulation is an increasingly sought-after strategy [2, 30].

Development and clinical application of Mg-based materials is impaired by Mg unpredictable corrosion in aqueous environments, hydrogen gas formation and pH alkalization during degradation [17, 18, 31]. Mg combination with polymers, may improve Mg corrosion resistance [32], and Fg regenerative properties, render it an attractive interface for Mg-based materials and host tissue. Thus, in this study Fg and

Mg were combined for the first time to make FgMg. The rational underlying this biomaterial combination was that Fg and Mg could act synergistically to modulate macrophage polarization and promote a pro-regenerative microenvironment. Herein, the Mg disc was surrounded by an upper and a lower Fg layer, aiming to provide a protective coating to Mg. The presence of Mg material did not alter the Fg layer porosity, which was similar to that previously reported for Fg scaffolds [12]. In the current work *in vitro* degradation rates of Fg, Mg and FgMg were indirectly evaluated, *via* the concentration of Mg^{2+} and D-dimer (Fg degradation product) in their extracts. Fg scaffolds were previously reported to be more susceptible to *in vitro* hydrolysis, than proteolysis [12]. For Mg-based biomaterials, correlations between *in vivo* and *in vitro* degradation rates are reported to be better achieved when biomaterials are immersed in cell culture media under physiological conditions (37 ºC, 21% O2, 5% CO2, 95% RH) [33]. Importantly, comparison between *in vitro* and *in vivo* degradation rates is not straightforward. Degradation rates determined *in vitro* allow only to infer a potential *in vivo* degradation pattern [34]. Protein adsorption upon biomaterial implantation, is known to condition the host inflammatory response and interactions with immune cells [35]. Fg is one of the most studied proteins for adsorption to biomaterials [36], being able to interact with other proteins. The Fg layer in FgMg is expected to facilitate interaction with host proteins and cells.

The current study used biomaterial extracts to evaluate the immunomodulatory impact of Fg, Mg and FgMg degradation products, particularly on primary human macrophages. This approach has been previously reported to evaluate the impact of Mg-based materials on different cell populations [15, 20, 37, 38], including on THP1-derived macrophages [39], but not primary human macrophages. Here, biomaterial extracts were diluted 10-fold, achieving a physiological pH, in agreement with previous recommendation on improving conditions for *in vitro* testing Mg-based materials [31, 40].

Stimulation of immune cells in buffy coats from peripheral blood of healthy blood donors was evaluated based on TNF-α secretion, as TNF-α is reported to be secreted in response to endotoxins, like LPS, in a concentration dependent-manner [22]. The biomaterial extracts *per se* did not promote TNF-α secretion, supporting low endotoxin content. When cells were stimulated with LPS, TNF-α secretion was impaired by the presence of biomaterials extracts, particularly for FgMg. These results were further supported by the cytokine profile observed herein for macrophages.

Depending on microenvironmental cues, macrophages can polarize towards a range of phenotypes, from pro-inflammatory M1 to anti-inflammatory M2 [3]. The classical pro-inflammatory LPS-IFNγ M1 stimulation [41] was performed for 72h, which leads to full cell maturation [16]. Cell surface expression of M1 marker (CD86) showed that extracts from FgMg combination materials impaired macrophage M1 polarization, more efficiently than those from Fg or Mg separately. None of the extracts promoted increased the M2 macrophage marker CD163, suggesting a reduction of M1 polarization, but that is not accompanied by increased M2 phenotype. Previous work using RAW 264.7-derived macrophages on Mg-treated titanium materials showed that release of Mg^{2+} led to decreased pro-inflammatory markers (CD86), but the authors report also increased anti-inflammatory molecules, (CD163 and CD206), in non-stimulated or LPS-stimulated conditions [42, 43].

Moreover, Mg ions from materials containing Mg [42, 43], their extracts [39] or Mg salts ($MgSO_4$) [44-46], have also been associated with decreased pro-inflammatory cytokines production, including TNF-α and IL-6. Similarly, we observed a tendency for Mg-containing biomaterials extracts, to reduce IL-6 and IL-12p70 secretion levels.

In line with results presented here, previous work from our group showed that Fg adsorbed to chitosan reduced macrophage activation and pro-inflammatory cytokine secretion, stimulating release of pro-osteogenic and angiogenic factors [9]. Conversely, soluble Fg has been reported to stimulate macrophages towards a pro-inflammatory

profile [47], and increase pro-inflammatory cytokines secretion by human monocytes [48], and mouse macrophages [47]. Interestingly, here macrophage response to Fg-biomaterials extracts was closer to the one observed for adsorbed Fg, rather than for its soluble form. Of the anti-inflammatory cytokines tested, IL-10 has been described as a M2 cytokine [49-51]. Nevertheless, in this work and previous ones [52-54], M1 polarized macrophages were shown as important IL-10 producers, which has been suggested as a regulatory mechanism [55]. Additionally, FgMg extracts promoted an increased TGF-β1 secretion, upon M1 stimulation. However, the role of this cytokine in regulating macrophages responses remains incompletely established [56].

Macrophage polarization depends on activation of signaling pathways involving MAPK and NF-kB, downstream of LPS-mediated TLR4 engagement [28, 57, 58]. Our previous work indicated that adsorbed Fg induced MAPK phosphorylation, and that LPS induced a phosphorylation peak 30 min upon stimulation [8]. However, herein Fg-biomaterial extracts did not promote JNK, ERK and p38 phosphorylation, or modify phosphorylation levels upon M1 stimulation. Although soluble Fg was reported to increased monocyte NF-kB p65 activity [48], we did not find Fg extract-mediated NF-kB p65 phosphorylation. Also, Mg^{2+}supplementation (Mg salts), has been shown to reduce NF-kB activation, with subsequent reduction of pro-inflammatory cytokine secretion, upon LPS stimulation with or without IFNγ, in RAW 264.7 cell line [46] and cord blood monocytes [44]. Among NF-kB family members, p65 is typically involved in inflammatory response, with increased phosphorylation of NF-kB p65 being associated to the pathogenesis of several chronic inflammatory diseases [59]. NF-kB inhibition studies have shown that p65 silencing reduced secretion of pro-inflammatory mediators, like IL-6 [60]. The current work showed that FgMg combination extracts inhibit M1-stimulated NF-kB p65 to a greater extent than those of individual materials, indicating a synergistic impact of Fg and Mg on macrophages.

To address the functional implication of exposure to the biomaterials extracts on macrophages, their crosstalk with MSC was probed. MSC can be isolated from several sources, including bone marrow, adipose tissue, peripheral blood, placenta or umbilical cord blood. However, the amount of MSC obtained, their proliferation and differentiation capacity differ [61]. Herein, MSC were isolated from bone marrow, the most widely used source, due to their involvement in the bone repair microenvironment. Macrophages are reported to influence MSC osteogenic differentiation, through cytokine secretion [4, 62-64]. ALP activity was used as a marker for osteogenesis differentiation, as this enzyme activity is transiently increased when MSC commit to the osteogenic lineage, peaking at 14 days of differentiation [65]. While some studies highlight the role of pro-inflammatory M1 macrophages [62, 63] in stimulating MSC osteogenic differentiation, others attribute this role to anti-inflammatory M2 macrophages [4, 64]. In the current study, macrophage exposure to biomaterial extracts had a greater impact than M1 polarization in their secretome promoting MSC ALP activity and mineral deposition. Interestingly, gene expression analysis at day 7 was not in agreement with ALP activity and alizarin red staining at day 14, showing low transcription activation of *RUNX2* and *ALP* by the secretome of macrophages in all conditions tested (Supplementary Fig. 2). Although the impact of the selected time point cannot be ruled out, this might also be dependent on different mechanisms of regulation of protein translation and activity [66], as reported by Rescigno et al, where short exposures to low frequency magnetic fields induced higher ALP activity, when compared with its mRNA expression [67].

Together, the results presented here provide a proof-of-concept of Fg and Mg synergistic impact on macrophage M1 response, and their crosstalk with MSC, supporting the potential of FgMg combination biomaterials to be further developed for bone tissue repair. Nevertheless, some important questions should be addressed in future work. In the biomaterial development, analyzing the implications of changing the

proportions between Fg and Mg in the final biomaterial or the presence of alloying elements in the Mg component could further improve the outcomes reported here. Also, the angiogenic potential of the FgMg combination should be investigated. Interestingly, previous work showed that incorporation of Fg in Ch materials stimulated angiogenesis in a critical size bone defect model, although an increased number of blood vessels did not directly correlate with bone repair [11]. Also, Mg extracts have been reported to increase human umbilical vein endothelial cells proliferation, under hypoxic conditions [20]. This effect was concentration-dependent, with low Mg concentrations (10 mM) increasing vascular smooth muscle cell proliferation and migration rate, and higher Mg concentrations (40-60 mM) inducing coagulation and inflammation [68]. Finally, future evaluation of this combination biomaterial *in vivo* will be essential to understand its capacity to dampen inflammation and promote bone repair, particularly in inflammatory conditions.

Conclusion

In conclusion, the present study reports, for the first time, the combination of Fg and Mg biomaterials and the impact of their degradation products on macrophages. The results presented support the hypothesis that Fg and Mg can act synergistically to reduce macrophage pro-inflammatory stimulation, and lead macrophages to promote MSC osteogenic differentiation. Hence, the combination of Fg and Mg rises as an interesting strategy to tune the initial inflammatory response, dampening the M1 macrophage response, to support bone repair.

Acknowledgments

This work was funded by NORTE-01-0145-FEDER-000012, NORTE 2020, under PORTUGAL 2020 Partnership Agreement, through ERDF; Mafalda

Bessa-Gonçalves and João Paulo Brás are funded by FCT PhD Programmes and by Programa Operacional Potencial Humano (POCH), BiotechHealth Programme (Doctoral Programme on Cellular and Molecular Biotechnology Applied to Health Sciences – reference PD/BI/128355/2017 and PD/BI/128356/2017, respectively), and through the PhD studentship PD/BD/135489/2018 and PD/BD/135490/2018, respectively. The authors thank Grifols SA for donating clinical grade fibrinogen; Daniela Silva for the technical and scientific support with SEM analysis (CEMUP); i3S Scientific Platform Translational Cytometry, member of the PPBI (PPBI-POCI-01-0145-FEDER-022122); Serviço de Ortopedia and Serviço de Imunohemoterapia, Centro Hospitalar Universitário de São João for donating bone marrow samples and buffy coats, respectively; Monika Lucszak (HZG) for their expert technical assistance in extracts characterization; Maria Inês Almeida for her help with gene expression analysis.

Conflicts of interest

There are no conflicts to declare.

Disclosure Statement

No competing financial interests exist.

References

[1] F. Loi, L.A. Cordova, J. Pajarinen, T.H. Lin, Z. Yao, S.B. Goodman, Inflammation, fracture and bone repair, Bone 86 (2016) 119-30.

[2] Z. Julier, A.J. Park, P.S. Briquez, M.M. Martino, Promoting tissue regeneration by modulating the immune system, Acta Biomater 53 (2017) 13-28.

[3] E. Mariani, G. Lisignoli, R.M. Borzi, L. Pulsatelli, Biomaterials: Foreign Bodies or Tuners for the Immune Response?, Int J Mol Sci 20(3) (2019).

[4] L. Gong, Y. Zhao, Y. Zhang, Z. Ruan, The Macrophage Polarization Regulates MSC Osteoblast Differentiation in vitro, Ann Clin Lab Sci 46(1) (2016) 65-71.

[5] L. Vi, G.S. Baht, H. Whetstone, A. Ng, Q. Wei, R. Poon, S. Mylvaganam, M. Grynpas, B.A. Alman, Macrophages promote osteoblastic differentiation in-vivo: implications in fracture repair and bone homeostasis, J Bone Miner Res 30(6) (2015) 1090-102.

[6] F. Scognamiglio, A. Travan, I. Rustighi, P. Tarchi, S. Palmisano, E. Marsich, M. Borgogna, I. Donati, N. de Manzini, S. Paoletti, Adhesive and sealant interfaces for general surgery applications, J Biomed Mater Res B Appl Biomater 104(3) (2016) 626-39.

[7] D. Davalos, K. Akassoglou, Fibrinogen as a key regulator of inflammation in disease, Semin Immunopathol 34(1) (2012) 43-62.

[8] M.I. Oliveira, M.L. Pinto, R.M. Goncalves, M.C.L. Martins, S.G. Santos, M.A. Barbosa, Adsorbed Fibrinogen stimulates TLR-4 on monocytes and induces BMP-2 expression, Acta Biomater 49 (2017) 296-305.

[9] J. Maciel, M.I. Oliveira, E. Colton, A.K. McNally, C. Oliveira, J.M. Anderson, M.A. Barbosa, Adsorbed fibrinogen enhances production of bone- and angiogenic-related factors by monocytes/macrophages, Tissue Eng Part A 20(1-2) (2014) 250-63.

[10] C.R. Almeida, D.P. Vasconcelos, R.M. Goncalves, M.A. Barbosa, Enhanced mesenchymal stromal cell recruitment via natural killer cells by incorporation of inflammatory signals in biomaterials, J R Soc Interface 9(67) (2012) 261-71.

[11] S.G. Santos, M. Lamghari, C.R. Almeida, M.I. Oliveira, N. Neves, A.C. Ribeiro, J.N. Barbosa, R. Barros, J. Maciel, M.C. Martins, R.M. Goncalves, M.A. Barbosa, Adsorbed fibrinogen leads to improved bone regeneration and correlates with differences in the systemic immune response, Acta Biomater 9(7) (2013) 7209-17.

[12] D.M. Vasconcelos, R.M. Goncalves, C.R. Almeida, I.O. Pereira, M.I. Oliveira, N. Neves, A.M. Silva, A.C. Ribeiro, C. Cunha, A.R. Almeida, C.C. Ribeiro, A.M. Gil, E. Seebach, K.L. Kynast, W. Richter, M. Lamghari, S.G. Santos, M.A. Barbosa, Fibrinogen scaffolds with immunomodulatory properties promote in vivo bone regeneration, Biomaterials 111 (2016) 163-178.

[13] B.J. Luthringer, F. Feyerabend, R. Willumeit-Romer, Magnesium-based implants: a mini-review, Magnes Res 27(4) (2014) 142-54.

[14] D.M. Vasconcelos, S.G. Santos, M. Lamghari, M.A. Barbosa, The two faces of metal ions: From implants rejection to tissue repair/regeneration, Biomaterials 84 (2016) 262-275.

[15] B.J. Luthringer, R. Willumeit-Romer, Effects of magnesium degradation products on mesenchymal stem cell fate and osteoblastogenesis, Gene 575(1) (2016) 9-20.

[16] M.D. Costantino, A. Schuster, H. Helmholz, A. Meyer-Rachner, R. Willumeit-Romer, B.J.C. Luthringer-Feyerabend, Inflammatory response to magnesium-based biodegradable implant materials, Acta Biomater 101 (2020) 598-608.

[17] M. Razavi, Y. Huang, Assessment of magnesium-based biomaterials: from bench to clinic, Biomater Sci 7(6) (2019) 2241-2263.

[18] D. Zhao, F. Witte, F. Lu, J. Wang, J. Li, L. Qin, Current status on clinical applications of magnesium-based orthopaedic implants: A review from clinical translational perspective, Biomaterials 112 (2017) 287-302.

[19] S.A. Sell, M.P. Francis, K. Garg, M.J. McClure, D.G. Simpson, G.L. Bowlin, Cross-linking methods of electrospun fibrinogen scaffolds for tissue engineering applications, Biomed Mater 3(4) (2008) 045001.

[20] L. Xu, R. Willumeit-Romer, B.J.C. Luthringer-Feyerabend, Effect of magnesium-degradation products and hypoxia on the angiogenesis of human umbilical vein endothelial cells, Acta Biomater (2019).

[21] N.A. Agha, F. Feyerabend, B. Mihailova, S. Heidrich, U. Bismayer, R. Willumeit-Romer, Magnesium degradation influenced by buffering salts in concentrations typical of in vitro and in vivo models, Mater Sci Eng C Mater Biol Appl 58 (2016) 817-25.

[22] M. Daneshian, S. von Aulock, T. Hartung, Assessment of pyrogenic contaminations with validated human whole-blood assay, Nat Protoc 4(12) (2009) 1709-21.

[23] A.R. Almeida, M. Bessa-Goncalves, D.M. Vasconcelos, M.A. Barbosa, S.G. Santos, Osteoclasts degrade fibrinogen scaffolds and induce mesenchymal stem/stromal osteogenic differentiation, Journal of biomedical materials research. Part A (2019).

[24] M.I. Almeida, A.M. Silva, D.M. Vasconcelos, C.R. Almeida, H. Caires, M.T. Pinto, G.A. Calin, S.G. Santos, M.A. Barbosa, miR-195 in human primary mesenchymal stromal/stem cells regulates proliferation, osteogenesis and paracrine effect on angiogenesis, Oncotarget 7(1) (2016) 7-22.

[25] D.M. Vasconcelos, C. Falentin-Daudre, D. Blanquaert, D. Thomas, P.L. Granja, V. Migonney, Role of protein environment and bioactive polymer grafting in the S. epidermidis response to titanium alloy for biomedical applications, Mater Sci Eng C Mater Biol Appl 45 (2014) 176-83.

[26] J.P. Bras, A.M. Silva, G.A. Calin, M.A. Barbosa, S.G. Santos, M.I. Almeida, miR-195 inhibits macrophages pro-inflammatory profile and impacts the crosstalk with smooth muscle cells, PLoS One 12(11) (2017) e0188530.

[27] A.F. Valledor, E. Sanchez-Tillo, L. Arpa, J.M. Park, C. Caelles, J. Lloberas, A. Celada, Selective roles of MAPKs during the macrophage response to IFN-gamma, J Immunol 180(7) (2008) 4523-9.

[28] K.M. Rao, MAP kinase activation in macrophages, J Leukoc Biol 69(1) (2001) 3-10.

[29] S.E. Headland, L.V. Norling, The resolution of inflammation: Principles and challenges, Semin Immunol 27(3) (2015) 149-60.

[30] R. Sridharan, A.R. Cameron, D.J. Kelly, C.J. Kearney, F.J. O'Brien, Biomaterial based modulation of macrophage polarization: a review and suggested design principles, Materials Today 18(6) (2015) 313-325.

[31] J. Wang, F. Witte, T. Xi, Y. Zheng, K. Yang, Y. Yang, D. Zhao, J. Meng, Y. Li, W. Li, K. Chan, L. Qin, Recommendation for modifying current cytotoxicity testing standards for biodegradable magnesium-based materials, Acta Biomater 21 (2015) 237-49.

[32] L.Y. Li, L.Y. Cui, R.C. Zeng, S.Q. Li, X.B. Chen, Y. Zheng, M.B. Kannan, Advances in functionalized polymer coatings on biodegradable magnesium alloys - A review, Acta Biomater 79 (2018) 23-36.

[33] A.H. Martinez Sanchez, B.J. Luthringer, F. Feyerabend, R. Willumeit, Mg and Mg alloys: how comparable are in vitro and in vivo corrosion rates? A review, Acta Biomater 13 (2015) 16-31.

[34] J.M. Anderson, Future challenges in the in vitro and in vivo evaluation of biomaterial biocompatibility, Regen Biomater 3(2) (2016) 73-7.

[35] R.M. Visalakshan, M.N. MacGregor, S. Sasidharan, A. Ghazaryan, A.M. Mierczynska-Vasilev, S. Morsbach, V. Mailander, K. Landfester, J.D. Hayball, K. Vasilev, Biomaterial Surface Hydrophobicity-Mediated Serum Protein Adsorption and Immune Responses, ACS Appl Mater Interfaces 11(31) (2019) 27615-27623.

[36] T.A. Horbett, Fibrinogen adsorption to biomaterials, Journal of biomedical materials research. Part A 106(10) (2018) 2777-2788.

[37] A.H. Martinez Sanchez, F. Feyerabend, D. Laipple, R. Willumeit-Romer, A. Weinberg, B.J.C. Luthringer, Chondrogenic differentiation of ATDC5-cells under the influence of Mg and Mg alloy degradation, Mater Sci Eng C Mater Biol Appl 72 (2017) 378-388.

[38] F. Cecchinato, N.A. Agha, A.H. Martinez-Sanchez, B.J. Luthringer, F. Feyerabend, R. Jimbo, R. Willumeit-Romer, A. Wennerberg, Influence of Magnesium Alloy Degradation on Undifferentiated Human Cells, PLoS One 10(11) (2015) e0142117.

[39] L. Jin, J. Wu, G. Yuan, T. Chen, In vitro study of the inflammatory cells response to biodegradable Mg-based alloy extract, PLoS One 13(3) (2018) e0193276.

[40] J. Fischer, D. Pröfrock, N. Hort, R. Willumeit, F. Feyerabend, Reprint of: Improved cytotoxicity testing of magnesium materials, Materials Science and Engineering: B 176(20) (2011) 1773-1777.

[41] M. Orecchioni, Y. Ghosheh, A.B. Pramod, K. Ley, Macrophage Polarization: Different Gene Signatures in M1(LPS+) vs. Classically and M2(LPS-) vs. Alternatively Activated Macrophages, Front Immunol 10 (2019) 1084.

[42] B. Li, H. Cao, Y. Zhao, M. Cheng, H. Qin, T. Cheng, Y. Hu, X. Zhang, X. Liu, In vitro and in vivo responses of macrophages to magnesium-doped titanium, Sci Rep 7 (2017) 42707.

[43] X. Li, Q. Huang, L. Liu, W. Zhu, T.A. Elkhooly, Y. Liu, Q. Feng, Q. Li, S. Zhou, Y. Liu, H. Wu, Reduced inflammatory response by incorporating magnesium into porous TiO2 coating on titanium substrate, Colloids Surf B Biointerfaces 171 (2018) 276-284.

[44] J. Sugimoto, A.M. Romani, A.M. Valentin-Torres, A.A. Luciano, C.M. Ramirez Kitchen, N. Funderburg, S. Mesiano, H.B. Bernstein, Magnesium decreases inflammatory cytokine production: a novel innate immunomodulatory mechanism, J Immunol 188(12) (2012) 6338-46.

[45] F. Gao, B. Ding, L. Zhou, X. Gao, H. Guo, H. Xu, Magnesium sulfate provides neuroprotection in lipopolysaccharide-activated primary microglia by inhibiting NF-kappaB pathway, J Surg Res 184(2) (2013) 944-50.

[46] T. Hu, H. Xu, C. Wang, H. Qin, Z. An, Magnesium enhances the chondrogenic differentiation of mesenchymal stem cells by inhibiting activated macrophage-induced inflammation, Sci Rep 8(1) (2018) 3406.

[47] J.Y. Hsieh, T.D. Smith, V.S. Meli, T.N. Tran, E.L. Botvinick, W.F. Liu, Differential regulation of macrophage inflammatory activation by fibrin and fibrinogen, Acta Biomater 47 (2017) 14-24.

[48] D.B. Kuhns, D.A. Priel, J.I. Gallin, Induction of human monocyte interleukin (IL)-8 by fibrinogen through the toll-like receptor pathway, Inflammation 30(5) (2007) 178-88.

[49] F.O. Martinez, S. Gordon, The M1 and M2 paradigm of macrophage activation: time for reassessment, F1000Prime Rep 6 (2014) 13.

[50] J.P. Edwards, X. Zhang, K.A. Frauwirth, D.M. Mosser, Biochemical and functional characterization of three activated macrophage populations, J Leukoc Biol 80(6) (2006) 1298-307.

[51] F.O. Martinez, A. Sica, A. Mantovani, M. Locati, Macrophage activation and polarization, Front Biosci 13 (2008) 453-61.

[52] F. Raggi, S. Pelassa, D. Pierobon, F. Penco, M. Gattorno, F. Novelli, A. Eva, L. Varesio, M. Giovarelli, M.C. Bosco, Regulation of Human Macrophage M1-M2 Polarization Balance by Hypoxia and the Triggering Receptor Expressed on Myeloid Cells-1, Front Immunol 8 (2017) 1097.

[53] A.A. Tarique, J. Logan, E. Thomas, P.G. Holt, P.D. Sly, E. Fantino, Phenotypic, functional, and plasticity features of classical and alternatively activated human macrophages, Am J Respir Cell Mol Biol 53(5) (2015) 676-88.

[54] M. Jaguin, N. Houlbert, O. Fardel, V. Lecureur, Polarization profiles of human M-CSF-generated macrophages and comparison of M1-markers in classically activated macrophages from GM-CSF and M-CSF origin, Cell Immunol 281(1) (2013) 51-61.

[55] W.A. Baseler, L.C. Davies, L. Quigley, L.A. Ridnour, J.M. Weiss, S.P. Hussain, D.A. Wink, D.W. McVicar, Autocrine IL-10 functions as a rheostat for M1 macrophage glycolytic commitment by tuning nitric oxide production, Redox Biol 10 (2016) 12-23.

[56] A. Kelly, S. Gunaltay, C.P. McEntee, E.E. Shuttleworth, C. Smedley, S.A. Houston, T.M. Fenton, S. Levison, E.R. Mann, M.A. Travis, Human monocytes and macrophages regulate immune tolerance via integrin alphavbeta8-mediated TGFbeta activation, J Exp Med 215(11) (2018) 2725-2736.

[57] H. Chi, S.P. Barry, R.J. Roth, J.J. Wu, E.A. Jones, A.M. Bennett, R.A. Flavell, Dynamic regulation of pro- and anti-inflammatory cytokines by MAPK phosphatase 1 (MKP-1) in innate immune responses, Proc Natl Acad Sci U S A 103(7) (2006) 2274-9.

[58] M.G. Dorrington, I.D.C. Fraser, NF-kappaB Signaling in Macrophages: Dynamics, Crosstalk, and Signal Integration, Front Immunol 10 (2019) 705.

[59] S. Giridharan, M. Srinivasan, Mechanisms of NF-kappaB p65 and strategies for therapeutic manipulation, J Inflamm Res 11 (2018) 407-419.

[60] U.J. Lee, S.R. Choung, K.V. Prakash, E.J. Lee, M.Y. Lee, Y.J. Kim, C.W. Han, Y.C. Choi, Dual knockdown of p65 and p50 subunits of NF-kappaB by siRNA inhibits the induction of inflammatory cytokines and significantly enhance apoptosis in human primary synoviocytes treated with tumor necrosis factor-alpha, Mol Biol Rep 35(3) (2008) 291-8.

[61] R. Hass, C. Kasper, S. Bohm, R. Jacobs, Different populations and sources of human mesenchymal stem cells (MSC): A comparison of adult and neonatal tissue-derived MSC, Cell Commun Signal 9 (2011) 12.

[62] P. Guihard, Y. Danger, B. Brounais, E. David, R. Brion, J. Delecrin, C.D. Richards, S. Chevalier, F. Redini, D. Heymann, H. Gascan, F. Blanchard, Induction of osteogenesis in mesenchymal stem cells by activated monocytes/macrophages depends on oncostatin M signaling, Stem Cells 30(4) (2012) 762-72.

[63] L.Y. Lu, F. Loi, K. Nathan, T.H. Lin, J. Pajarinen, E. Gibon, A. Nabeshima, L. Cordova, E. Jamsen, Z. Yao, S.B. Goodman, Pro-inflammatory M1 macrophages promote Osteogenesis by mesenchymal stem cells via the COX-2-prostaglandin E2 pathway, J Orthop Res 35(11) (2017) 2378-2385.

[64] Y. Zhang, T. Bose, R.E. Unger, J.A. Jansen, C.J. Kirkpatrick, J. van den Beucken, Macrophage type modulates osteogenic differentiation of adipose tissue MSCs, Cell Tissue Res 369(2) (2017) 273-286.

[65] E. Birmingham, G.L. Niebur, P.E. McHugh, G. Shaw, F.P. Barry, L.M. McNamara, Osteogenic differentiation of mesenchymal stem cells is regulated by osteocyte and osteoblast cells in a simplified bone niche, Eur Cell Mater 23 (2012) 13-27.

[66] C. Vogel, E.M. Marcotte, Insights into the regulation of protein abundance from proteomic and transcriptomic analyses, Nat Rev Genet 13(4) (2012) 227-32.

[67] T. Rescigno, A. Capasso, B. Bisceglia, M.F. Tecce, Short Exposures to an Extremely Low-Frequency Magnetic Field (ELF MF) Enhance Protein but not mRNA Alkaline Phosphatase Expression in Human Osteosarcoma Cells, Open Biochem J 12 (2018) 65-77.

[68] J. Ma, N. Zhao, D. Zhu, Biphasic responses of human vascular smooth muscle cells to magnesium ion, Journal of biomedical materials research. Part A 104(2) (2016) 347-56.

Figure Legends:

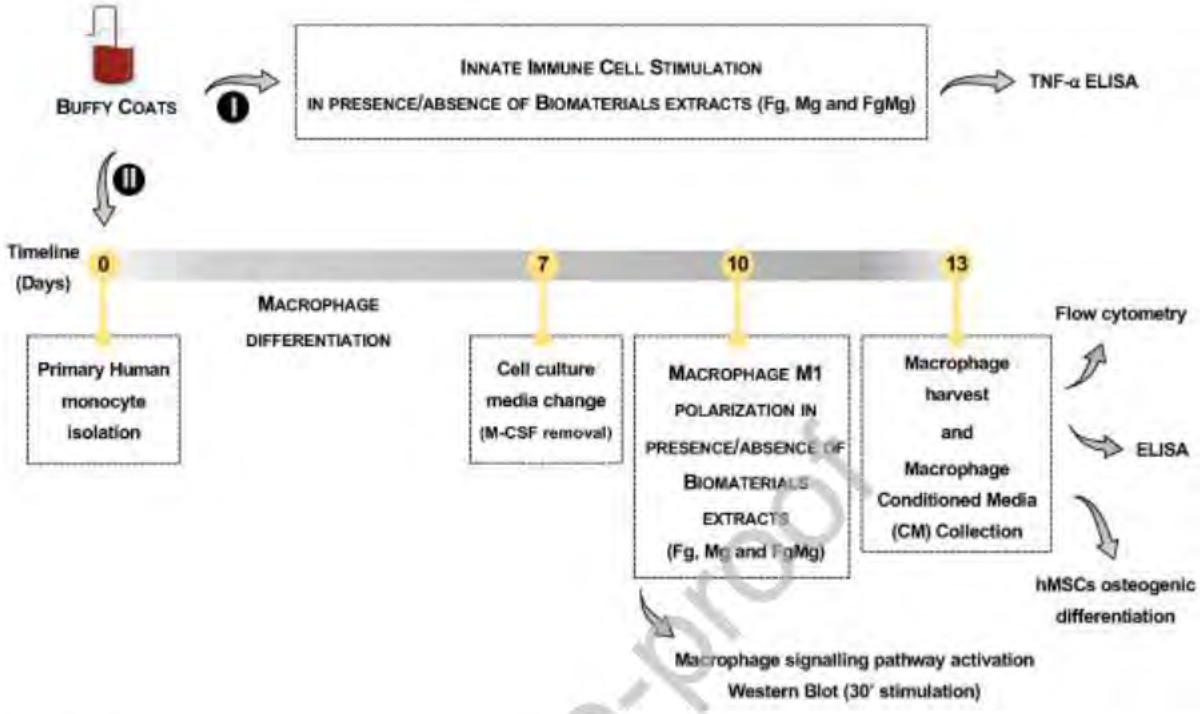

Fig. 1. Experimental timeline and readouts

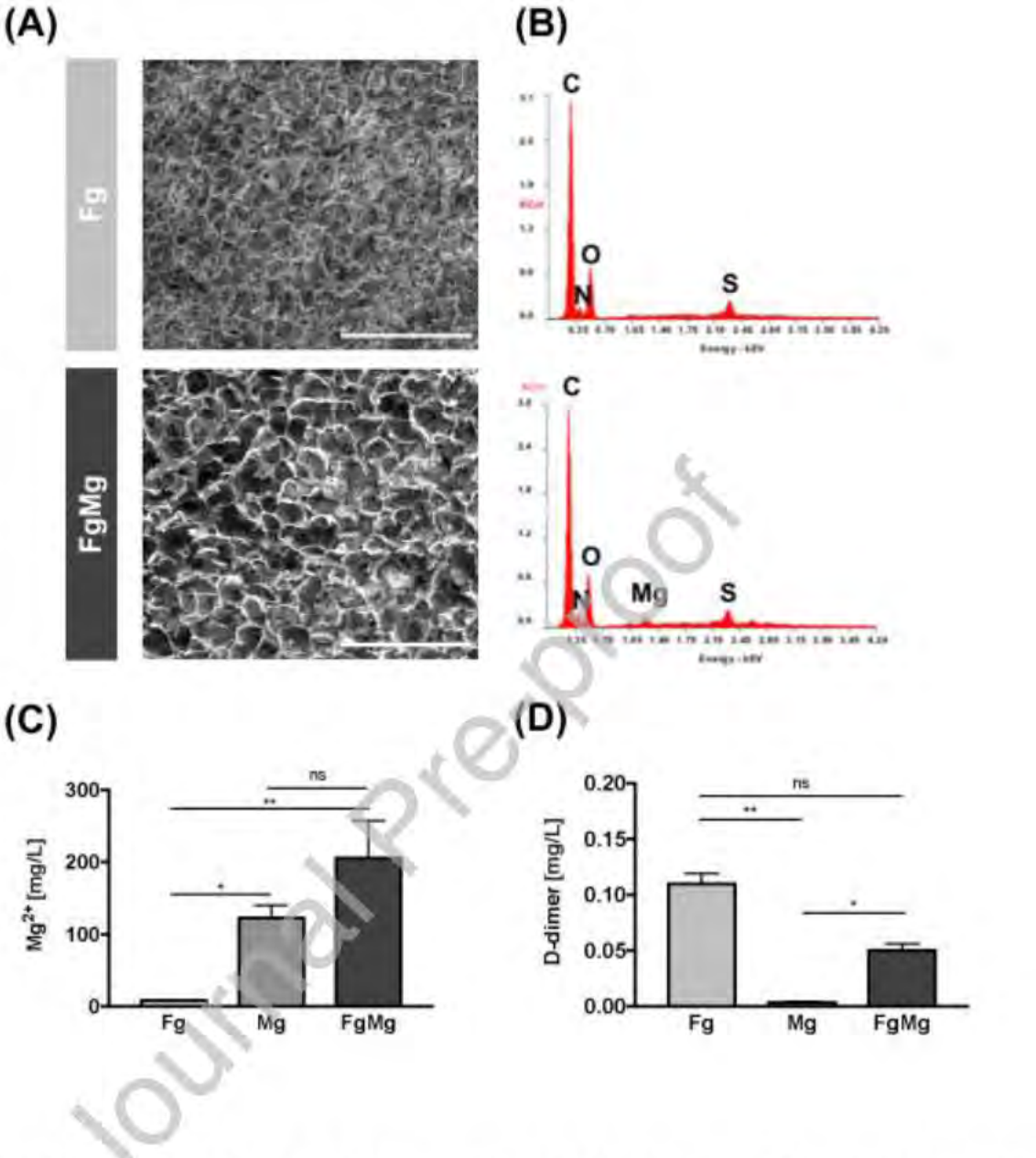

Fig. 2. Morphology of Fg alone or combined with Mg discs and biomaterials extracts composition. (A) SEM evaluation of the porous structure and (B) surface elemental composition of Fg alone or from FgMg combination (C: carbon, N: nitrogen, O: oxygen, Mg: magnesium, S: sulfur). Magnification: 250x. Scale bar: 400 µm. (C) Concentration of Mg2+ ions and (D) Fg-derived D-dimer in pure extracts. Data represent arithmetic mean ± SD, analyzed by Kruskal-Wallis test followed by uncorrected Dunn's test (n=3). *p<0.05; **p<0.01.

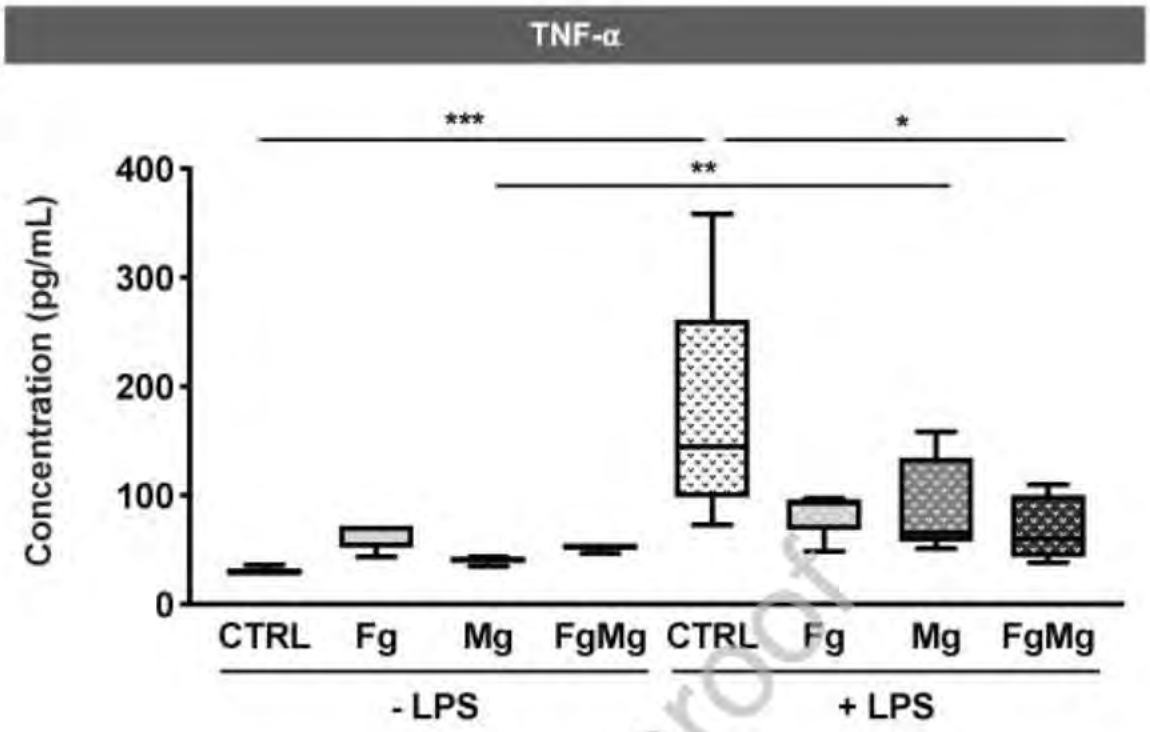

Fig. 3. TNF-α secretion levels in buffy coats stimulated with Fg, Mg and FgMg extracts alone or in the presence of LPS. Innate immune cells in buffy coats were left unstimulated or stimulated with LPS in presence/absence of biomaterials extracts (Fg, Mg and FgMg extracts). TNF-α secretion was determined by ELISA. Graphs are minimum to maximum box-and-whiskers plots, with median representation (n=5 independent donors). Friedman's test followed by uncorrected Dunn's test was performed. *p<0.05; **p<0.01; ***p<0.001.

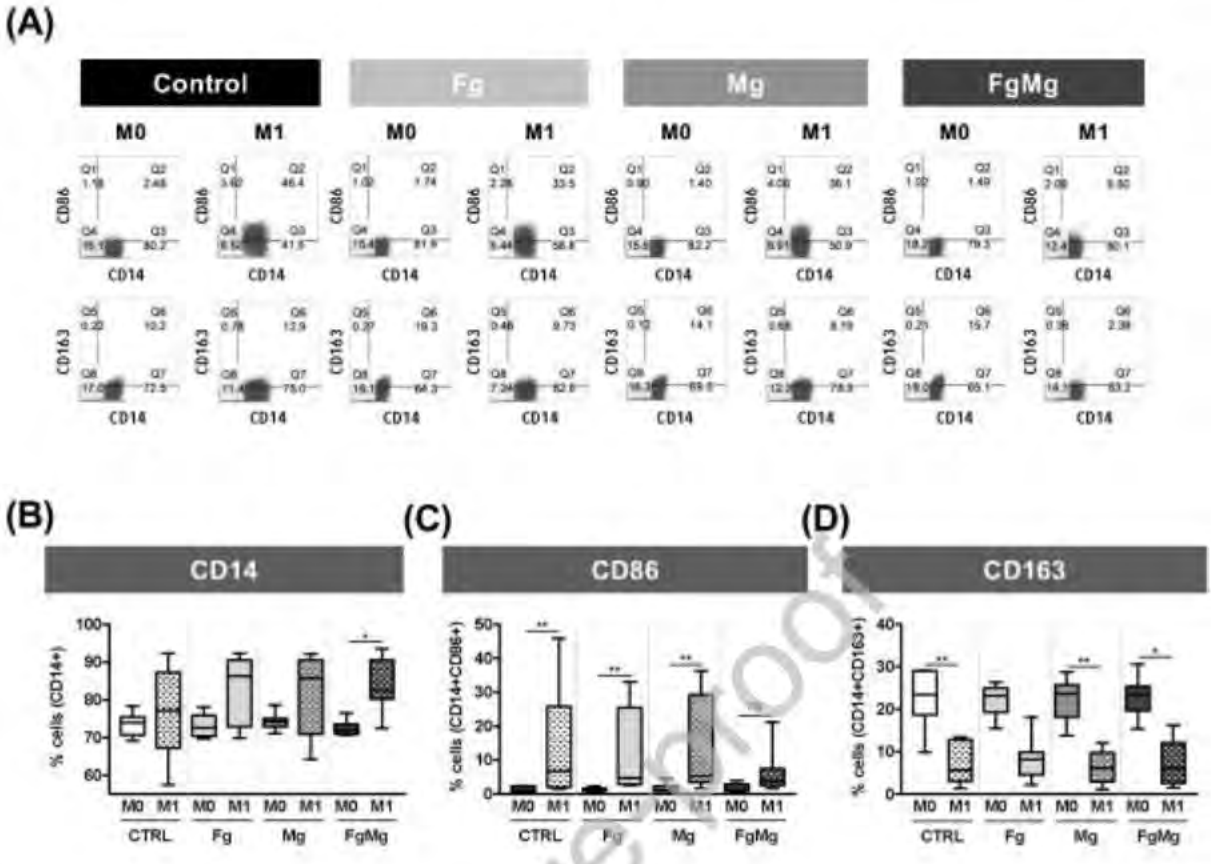

Fig. 4. Macrophage cell surface receptor profile upon preconditioning with Fg, Mg and FgMg extracts in the presence/absence of M1 stimulation. Macrophages were cultured with Fg, Mg and FgMg extracts with or without M1 stimulation (LPS-IFNγ) for 72 h, before being harvested, stained for the indicated cell surface markers and analyzed by flow cytometry. (A) Dot plots of a representative blood donor, where values in each quadrant represent percentage of cells in that quadrant (B) Percentage of CD14+ cells (n=8). (C) Percentage of double-positive cells, CD14+CD86+ (n=8). (D) Percentage of double-positive cells, CD14+CD163+ (n=8). Isotype controls were used to define background staining. M0=naïve/unstimulated macrophages; M1=LPS-IFNγ stimulated macrophages. Graphs are minimum to maximum box-and-whiskers plots, with median representation. Friedman's test followed by corrected Dunn's test were performed. *p<0.05; **p<0.01.

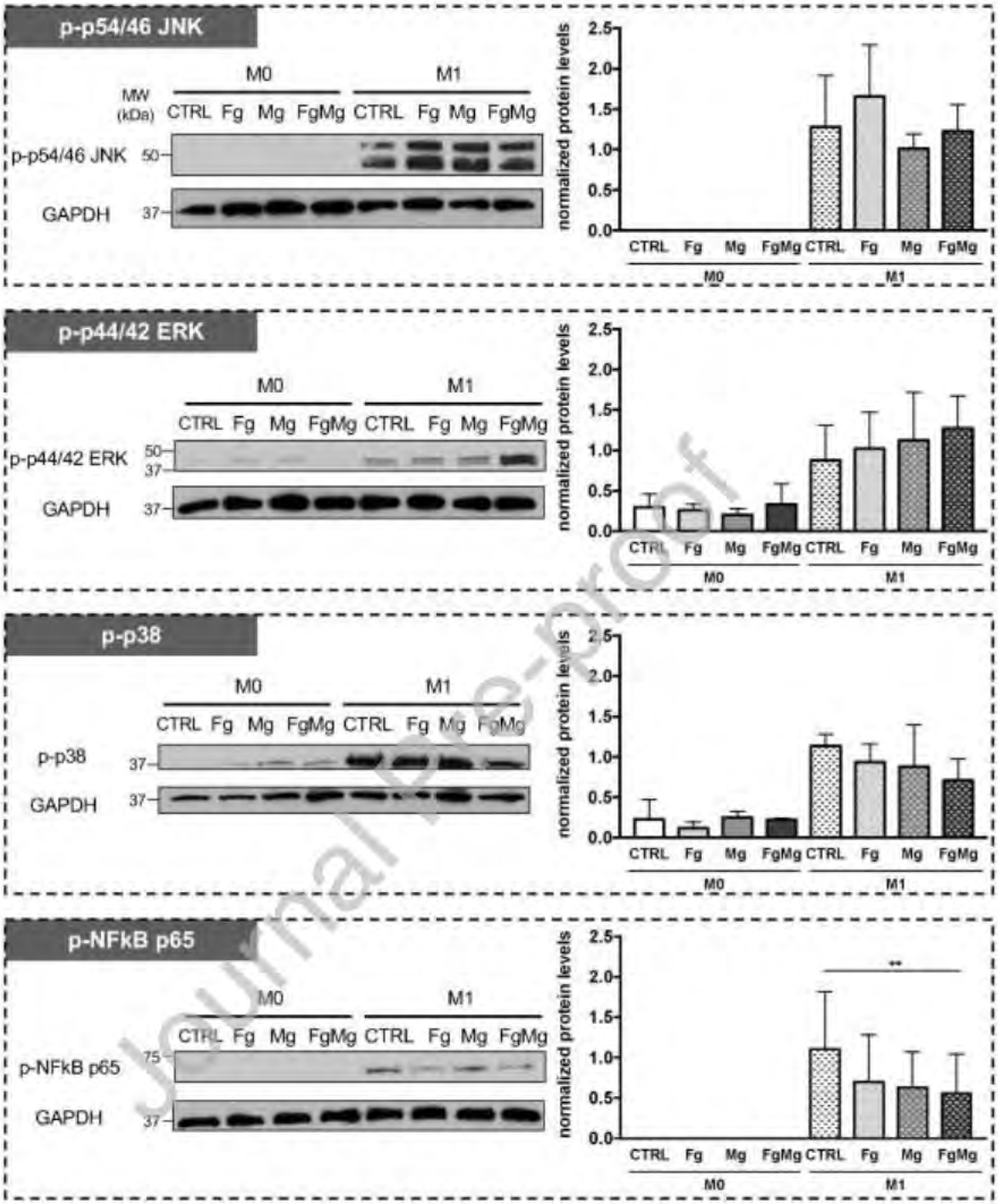

Fig. 5. Activation of MAPK (JNK, ERK, p38) and NF-kB p65 signalling pathways in macrophages preconditioned with Fg, Mg and FgMg extracts with or without M1 stimulation. Western blot shows protein levels of p54/46 JNK, p44/42 ERK, p38 and NF-kB p65 phosphorylated forms in macrophages preconditioned with or without (CTRL) biomaterials extracts (Fg, Mg and FgMg extracts) in the presence/absence (M0) of M1

stimulation (LPS-IFNγ). p-p54/46 JNK (n=3), p-p44/42 ERK (n=3), p-p38 (n=3) and p-NF-kB p65 (n=4) Relative protein levels were quantified using Image Lab software. GAPDH was used as normalizer. Data are mean ± SD. Friedman's test followed by corrected Dunn's test were performed. **p<0.01.

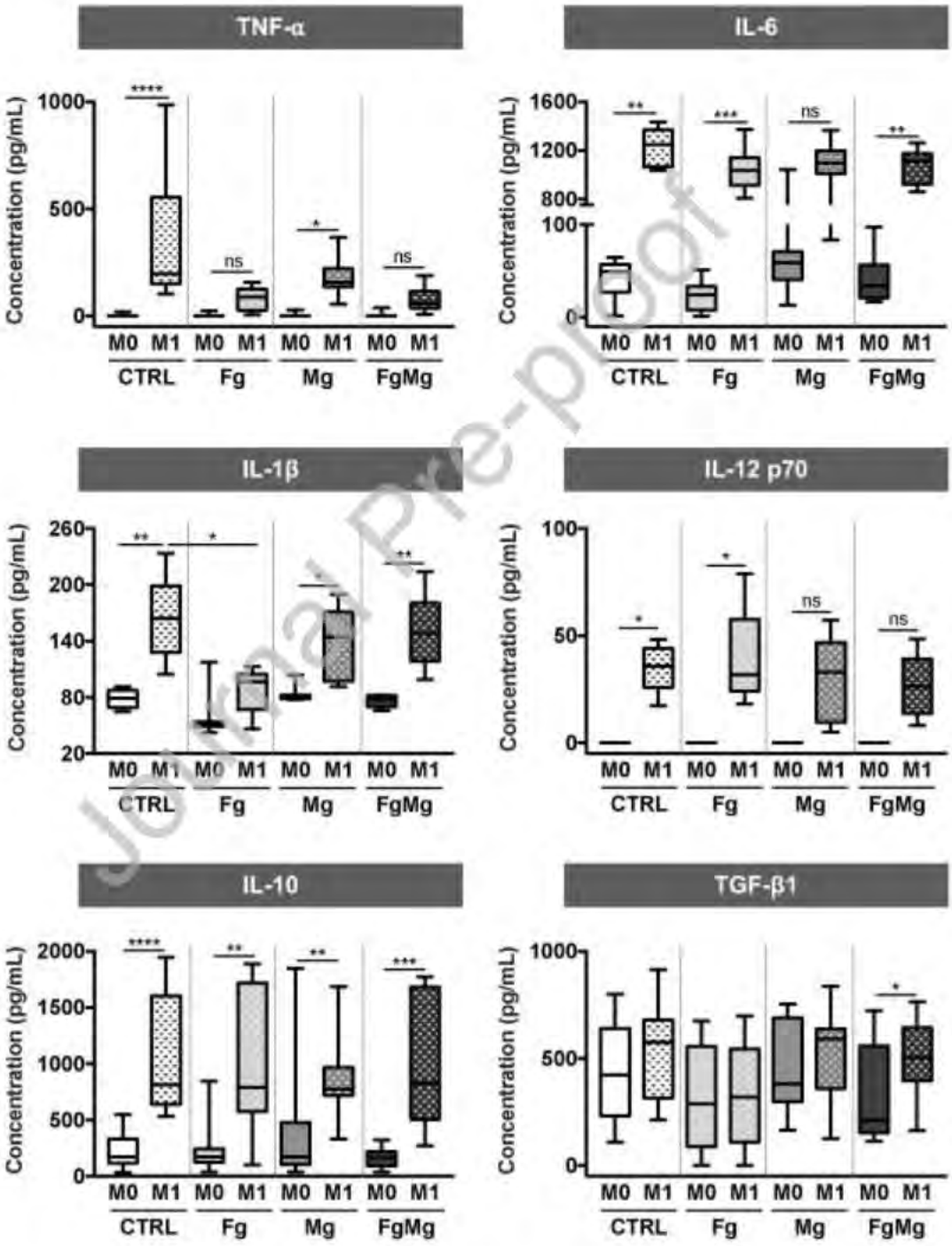

Fig. 6. Macrophage cytokine production upon preconditioning with Fg, Mg and FgMg extracts alone or in the presence of M1 stimulation. TNF-α, IL-6, IL-1β, IL-12p70, IL-10 and TGF-β1 release were determined by ELISA using macrophages secretome at day 13, from the following conditions: M0=naïve/unstimulated macrophages; M1=LPS-IFNγ stimulated macrophages; and macrophages preconditioned with Fg, Mg and FgMg extracts in the presence/absence of M1 stimulation. Graphs are minimum to maximum box-and-whiskers plots, with median representation. Friedman's test followed by corrected Dunn's multiple comparisons was performed for TNF-α, IL-6, IL-1β (all n=8), IL-12p70 (n=5) and IL-10 (n=11). One-way ANOVA followed by Sidak's multiple comparisons test was performed for TGF-β1 (n=11). *p<0.05; **p<0.01; ***p<0.001; ****p<0.0001.

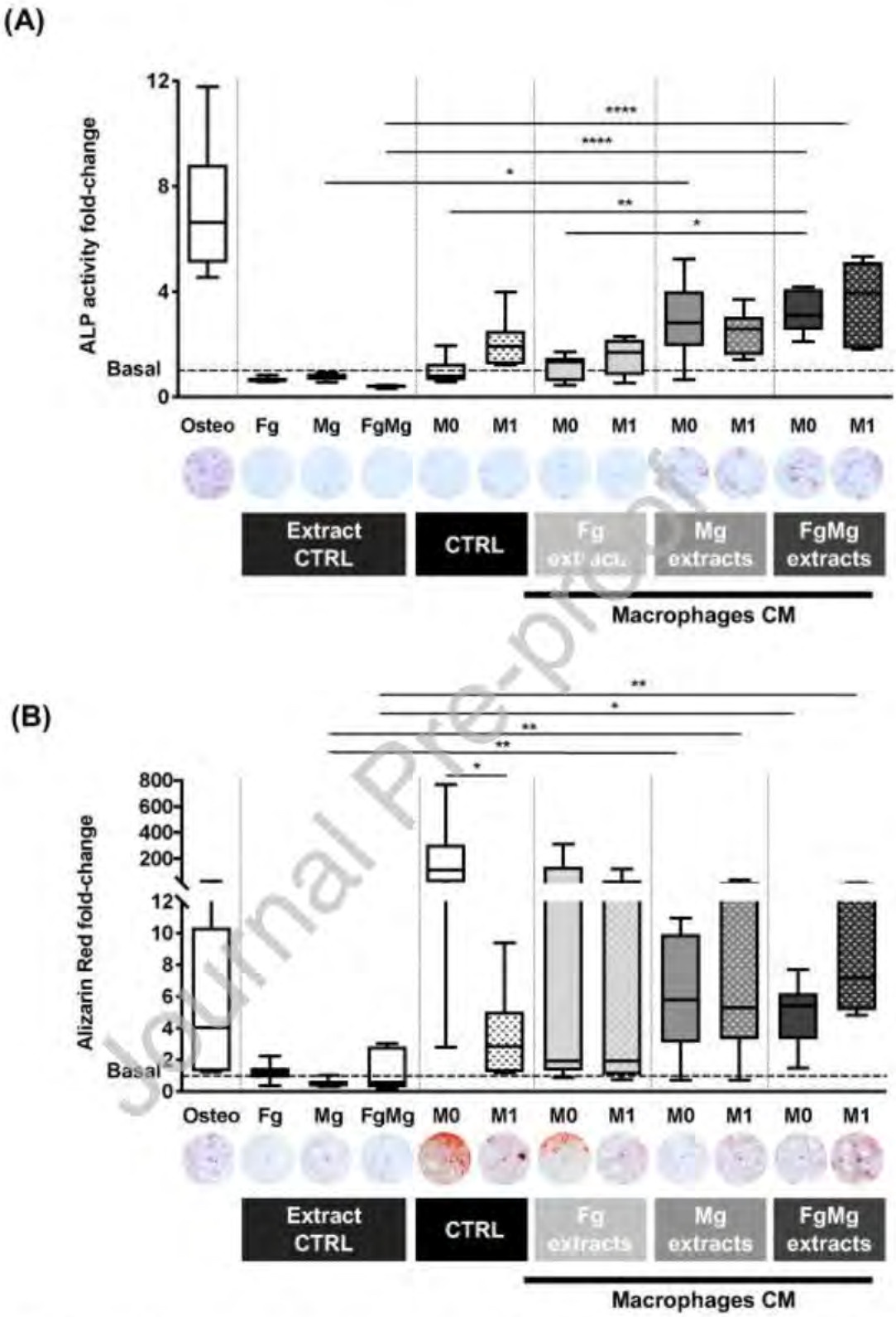

Fig.7. Effect of macrophage secretome on MSC osteogenic differentiation. MSC were incubated for 14 days with biomaterial extracts (extract CTRL= Fg, Mg and FgMg biomaterials extracts) or the secretome of macrophages unstimulated (M0), or LPS-IFNγ

stimulated (M1), in presence/absence of biomaterial extracts (CTRL=conditioned media from macrophages not exposed to extracts; Fg, Mg and FgMg extracts=conditioned media from macrophages preconditioned with Fg, Mg and FgMg extracts alone), as indicated. Basal and osteogenic (osteo) media were used as controls. ALP (A) and Alizarin Red (B) stainings were performed and stained areas were quantified using MATLAB. Values were normalized by the basal condition (n=6). Representative pictures (Zoom=1.6x) are shown for each condition. Error bars on box-and-whiskers plots indicate the minimum and maximum values, with median representation. Friedman's test followed by uncorrected Dunn's test were performed. *p<0.05; **p<0.01; ****p<0.0001.

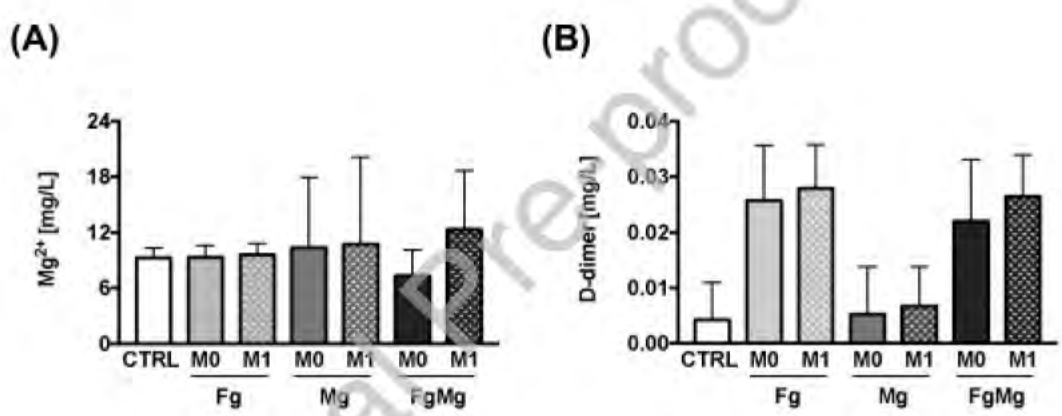

Fig. 8. Magnesium and fibrinogen degradation products content in conditioned media from macrophages cultured with Fg, Mg and FgMg extracts in the presence/absence of M1 stimulation. (A) Mg content and (B) Fg degradation products (D-dimer) in conditioned media from macrophages preconditioned with biomaterials extracts (Fg, Mg and FgMg) alone or in the presence of M1 stimulation (LPS-IFNγ). Data are mean ± SD. Friedman's test followed by corrected Dunn's test were performed for conditioned media measurements (n=8).

Graphical Abstarct